mining

MDPI

Article

Enhanced Hydrometallurgical Recovery of Copper from Balkhash Copper Concentrate Through High-Energy Milling

Lyazzat A. Mussapyrova [1,2], Ainur Sh. Aubakir [2], Magzhan T. Ysksk [1], Aisulu N. Batkal [1,2] and Kaster Kamunur [1,2,*]

[1] Institute of Combustion Problems, Almaty 050012, Kazakhstan; abatkalova@mail.ru (A.N.B.)
[2] Faculty of Chemistry and Chemical Technology, Al-Farabi Kazakh National University, Almaty 050040, Kazakhstan
* Correspondence: kkamunur@gmail.com

Abstract

This study investigated the influence of high-energy milling and leaching conditions on copper extraction from an industrial copper concentrate obtained from the Balkhash copper smelter. The concentrate was subjected to high-energy milling in a planetary ball mill for 15, 30, 45, and 60 min, followed by leaching in ammonium hydroxide and citric acid solutions. The structural, morphological, and physical changes induced by milling were evaluated using X-ray diffraction (XRD), scanning electron microscopy (SEM), particle-size distribution (PSD), and Brunauer–Emmett–Teller (BET) specific surface area analysis. XRD analysis showed that the principal mineral phases, including chalcopyrite, quartz, copper sulfides, magnetite, and lead sulfate, remained detectable after milling, whereas changes in diffraction peak shape and relative intensity indicated modification of the structural state of the concentrate. SEM observations demonstrated progressive disruption and fragmentation of the initial coarse particles. Quantitative particle-size analysis confirmed substantial particle refinement, with the D50 and D90 values decreasing from 5.030 and 57.365 μm for the untreated concentrate to 1.193 and 5.101 μm, respectively, after 30 min of milling. The BET specific surface area increased from 0.5086 m^2/g for the untreated concentrate to a maximum of 1.7801 m^2/g after 30 min, followed by a non-monotonic variation at longer milling times. Under the selected leaching conditions, copper extraction from the untreated concentrate reached 67% in ammonium hydroxide solution and 77% in citric acid solution. High-energy milling further increased copper extraction to 81% after 45 min in ammonium hydroxide and to 86% after 60 min in citric acid. The combined XRD, SEM, PSD, and BET results demonstrate that high-energy milling substantially modified the structural, morphological, particle-size, and accessible surface characteristics of the concentrate. However, the different milling durations corresponding to the maximum BET surface area and maximum copper extraction indicate that enhanced leaching performance cannot be attributed to surface-area enlargement alone and is associated with the combined effects of particle fragmentation, accessible surface-area changes, and milling-induced structural modification.

Keywords: copper concentrate; high-energy milling; hydrometallurgy; particle-size distribution; BET specific surface area; leaching; ammonium hydroxide; citric acid; copper extraction

Check for updates

Academic Editor: Mostafa Benzaazoua

Received: 10 September 2026
Revised: 16 October 2026
Accepted: 23 October 2026
Published: 27 October 2026

Copyright: © 2026 by the authors. Licensee MDPI, Basel, Switzerland. This article is an open access article distributed under the terms and conditions of the Creative Commons Attribution (CC BY) license.

1. Introduction

Today, copper is considered one of the most strategically important non-ferrous metals in the global economy. Due to its high electrical conductivity, excellent corrosion resistance and favorable technological properties, copper is widely used in the electrical and electronics industry, mechanical engineering, construction, energy systems and renewable energy technologies. The rapid growth of electric vehicle production, the modernization of energy infrastructure and the increasing demand for high-tech products have led to a continuous increase in global copper consumption [1]. Consequently, increasing copper production and improving the efficiency of using existing mineral resources are key scientific and technological challenges.

Currently, most copper concentrates are processed pyrometallurgically [2]. Although pyrometallurgical treatment is industrially established and efficient, it generally requires high-temperature operation and produces sulfur dioxide (SO_2), necessitating effective off-gas treatment. In contrast, hydrometallurgical methods operate at relatively low temperatures and can selectively dissolve valuable metals, providing potential advantages in terms of process flexibility, energy demand, and environmental impact. They can also reduce the need for high-temperature furnaces and associated gas-cleaning infrastructure, which may be economically advantageous for appropriately selected feedstocks and process configurations. However, these potential benefits must be balanced against reagent consumption, leachate treatment, solid–liquid separation, and the energy requirements of mechanical pretreatment. Therefore, hydrometallurgy should not be considered universally more economical or environmentally benign, but rather as a complementary processing route whose advantages depend on the characteristics of the concentrate and the process configuration [3,4].

In recent years, the high-energy milling of mineral raw materials has established itself as one of the most promising approaches to intensifying hydrometallurgical processes. Mechanochemical treatment promotes the formation of structural defects in solid phases, the splitting of the crystal lattice, an increase in dispersion and an increase in the specific surface area [5,6]. These modifications increase the chemical reactivity of minerals and facilitate their interaction with leaching reagents [7]. In addition, mechanical activation leads to fragmentation of mineral aggregates and weakens the bond between valuable metals and the mineral matrix, which improves the efficiency of subsequent hydrometallurgical processing. Although the effects of high-energy milling for various mineral systems have been extensively studied [8–10], the structural changes that occur during the processing of copper concentrates and their influence on leaching behavior have not yet been fully elucidated. In particular, the complex mineralogical composition of industrial copper concentrates makes it difficult to generalize the present research results. Therefore, studying the physicochemical changes associated with high-energy milling of industrial copper concentrates and evaluating their relationship with metal recovery efficiency are of considerable scientific and practical importance. Kazakhstan is one of the world's leading copper-producing countries. The Balkhash Copper Smelting Plant, one of the largest metallurgical enterprises in the country, processes copper concentrates with diverse mineralogical compositions. In addition to copper-bearing minerals, these concentrates contain iron, silica, and other associated components that may significantly influence the efficiency of hydrometallurgical processes. Therefore, investigating the processing characteristics of copper concentrates obtained from the Balkhash Copper Smelting Plant is of considerable industrial and scientific importance [11–13].

This study aims to evaluate the influence of high-energy milling and leaching conditions on copper extraction from an industrial copper concentrate obtained from the Balkhash copper smelter. Structural, morphological, and particle-size changes associated with milling were examined using XRD, SEM, laser diffraction, and BET specific surface area analysis, while the effects of milling duration and leaching conditions were evaluated in ammonium hydroxide and citric acid solutions. Particular attention was given to establishing experimentally observed relationships between milling-induced changes and copper extraction without assigning these effects to mechanisms that were not quantitatively characterized.

2. Materials and Methods

2.1. Research Material

An industrial copper concentrate from the Balkhash copper smelter in Balkhash, Kazakhstan, was used as the raw material for this study. The concentrate consisted predominantly of copper sulfide minerals as well as iron- and silicon-containing compounds. Before the experimental studies, the concentrate was oven-dried, subjected to sieve analysis, and the fraction with a particle size of less than 100 μm was collected. The selected fraction was then thoroughly homogenized to ensure representative characterization and reproducible experimental results. The initial copper concentrate was examined by energy-dispersive X-ray spectroscopy coupled with scanning electron microscopy to identify the elements present in the analyzed regions. The detected elements are summarized in Table 1. Copper was the predominant element detected by SEM–EDS, together with oxygen, silicon, sulfur, iron, magnesium, aluminum, and lead.

Table 1. Elements detected in the initial copper concentrate by SEM–EDS.

Element	O	Mg	Al	Si	S	Fe	Cu	Pb
wt.%	24.36	0.37	1.95	10.39	8.49	5.02	41.21	1.83

Note: The SEM–EDS data are provided for qualitative/semi-quantitative elemental identification and should not be considered representative of the bulk chemical composition of the heterogeneous copper concentrate.

The presence of Fe and S is associated with copper–iron sulfide minerals, whereas Si and O originate mainly from quartz and oxide phases. Minor amounts of Pb, Mg and Al were also detected. The macroscopic appearance of the initial copper concentrate was documented using digital photography under ambient laboratory conditions before further sample preparation and characterization. The oxygen content detected by SEM–EDS (24.36 wt.%) should not be interpreted as direct evidence of secondary copper oxide minerals. Because SEM–EDS provides local, semi-quantitative elemental information, the detected oxygen may originate from quartz, iron-bearing oxide phases, and other oxygen-containing constituents of the heterogeneous concentrate. The XRD analysis did not identify distinct secondary copper oxide phases among the detectable crystalline phases of the initial concentrate. However, the presence of minor or poorly crystalline copper oxide phases cannot be definitively excluded using the available data. Therefore, the oxygen content obtained by SEM–EDS is not used to infer the presence or quantify the abundance of secondary copper oxide minerals. The corresponding photograph is presented in Figure 1a. The macroscopic appearance and XRD pattern of the initial copper concentrate are presented in Figure 1.

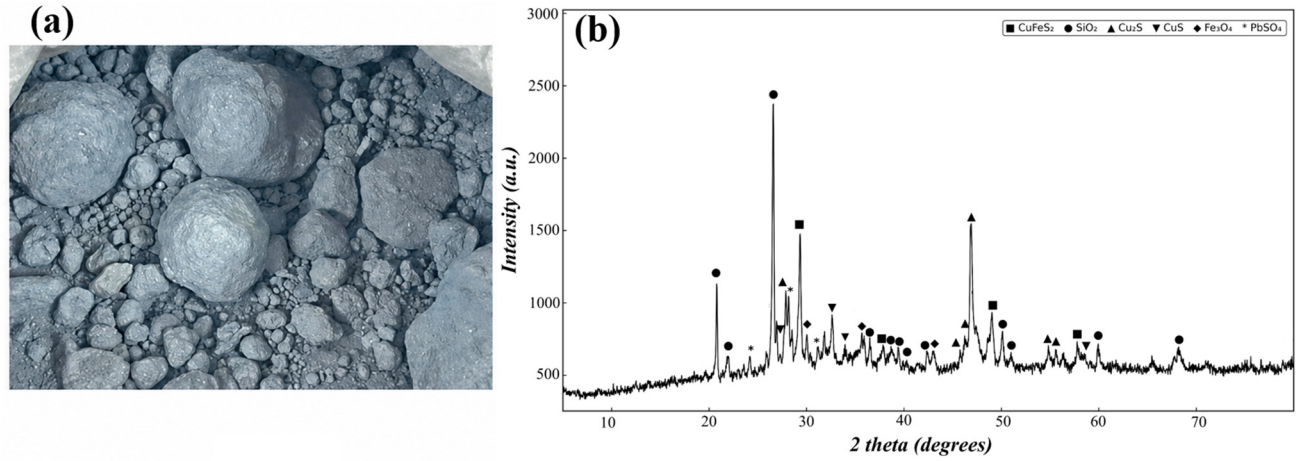


Figure 1. Digital photograph of the initial copper concentrate (**a**) and X-ray diffraction (XRD) pattern of the initial copper concentrate (**b**).

2.2. High-Energy Milling of Copper Concentrate

The copper concentrate was subjected to high-energy milling using a planetary ball mill (XQM, Changsha Tianchuang Powder Technology Co., Ltd., Changsha, China) equipped with a 250 mL stainless-steel grinding jar and stainless-steel balls with a total mass of 200 g. Milling was performed under ambient atmospheric conditions (air) without an inert atmosphere. The ball-to-powder mass ratio was 20:1, and the milling speed was maintained at 500 rpm. The samples were milled for 15, 30, 45, and 60 min under dry conditions without the addition of chemical reagents. Morphological changes associated with milling were evaluated qualitatively by SEM, while structural changes were examined by XRD. Because milling was conducted under ambient air using stainless-steel milling media, the possible effects of surface oxidation and contamination from the milling equipment were considered. However, quantitative measurements of Fe, Cr, and Ni originating from the milling media, as well as direct measurements of media wear or mass loss, were not performed in the present experimental campaign. Therefore, the possible contribution of these effects cannot be quantitatively excluded and is considered a limitation of the present study.

2.3. Structural, Phase, and Morphological Characterization

The phase composition and morphological characteristics of the untreated and milled copper concentrates, as well as the solid residues obtained after leaching, were characterized by X-ray diffraction (XRD) and scanning electron microscopy (SEM). XRD analyses were performed using a DRAWELL DW-XRD-27 mini diffractometer (Drawell, Shanghai, China) with Cu-Kα radiation ($\lambda = 1.5406$ Å). The diffraction patterns were recorded over a 2θ range of 10–90°, with a step size of 0.02° and a scanning rate of 2° min^{-1}. The morphology and particle shape of the samples, together with qualitative changes in particle fragmentation during high-energy milling and subsequent leaching, were examined using a Quanta 200i 3D scanning electron microscope (FEI, Hillsboro, OR, USA). XRD and SEM were used to evaluate structural and morphological changes associated with high-energy milling and leaching. The specific surface area of the untreated and high-energy-milled copper concentrate samples was determined by nitrogen adsorption–desorption measurements using an SSA-7000 automatic specific surface area and pore size analyzer. The measurements were performed using the vacuum static volumetric method, and the specific surface area was calculated according to the Brunauer–Emmett–Teller (BET) method. Nitrogen adsorption–desorption isotherms were recorded to evaluate changes in the accessible specific surface area of the concentrate induced by high-energy milling. Particle-size distribu-

tions of the untreated and high-energy-milled copper concentrate samples were determined by laser diffraction using a Winner 2005A particle-size analyzer (Jinan Winner Particle Instrument Stock Co., Ltd., Jinan, China). The analysis was used to quantitatively characterize the changes in particle size induced by high-energy milling. The particle-size distributions were evaluated in terms of the characteristic D10, D50, and D90 values, representing the particle diameters below which 10%, 50%, and 90% of the measured particle population were distributed, respectively. The average particle size and distribution span were also determined.

2.4. Acid–Alkaline Leaching Procedure

The hydrometallurgical behavior of the untreated and high-energy-milled copper concentrates was investigated using leaching experiments with ammonium hydroxide (NH_4OH) and citric acid ($C_6H_8O_7$). Ammonium hydroxide and citric acid were selected based on their different chemical functions and potential technological advantages. Ammonium hydroxide was chosen because ammonia forms stable ammine complexes with dissolved copper ions, particularly the tetraamminecopper (II) complex, thereby promoting copper dissolution and stabilizing copper in the liquid phase. An additional technological advantage of the ammoniacal system is the potential recovery and reuse of the complexing reagent. Ammonia may be recovered from the copper-bearing leach solution by thermal decomposition of the copper ammine complex or by ammonia stripping, absorbed in water, and subsequently reused in the leaching process. Such reagent recycling may reduce ammonia consumption and improve the environmental and economic performance of the process. Citric acid was selected as a biodegradable and relatively environmentally benign organic reagent. Its acidity facilitates the dissolution of copper-bearing mineral phases, while citrate ions form soluble complexes with dissolved copper and inhibit its reprecipitation. Therefore, ammonium hydroxide and citric acid were selected to compare a potentially recyclable alkaline complexing medium with an environmentally preferable organic-acid leaching system. The experiments were carried out in a thermostatically controlled 500 mL glass reactor. The leaching was carried out at temperatures of from 25 to 100 ° C. Over reaction times of from 30 to 180 min. No external oxidizing agent was added to either leaching system. The experiments were conducted under atmospheric air with continuous stirring at 500 rpm. However, pH, redox potential (Eh/ORP), and dissolved oxygen concentration were not monitored. Consequently, the redox conditions during leaching and the relative contributions of possible oxidation pathways could not be quantitatively established. The solid-to-liquid ratio (S/L) was maintained at 1:10 by mixing 5.00 g of copper concentrate with 50.0 mL (0.050 L) of the leaching solution. The suspension was stirred continuously at 500 rpm to ensure homogeneous mixing. After completion of the leaching, the suspension was filtered, the solid residues were thoroughly washed with distilled water and dried for subsequent characterization. The concentrations of the dissolved metals in the leaching water were determined and the metal yield was calculated according to the following equation:

$$R = \frac{C \cdot V}{m \cdot \alpha} \times 100 \quad (1)$$

where C is the metal concentration in the leaching solution (g L^{-1}), V is the volume of the leaching solution (L), m is the mass of the copper concentrate used for leaching (g), and α is the metal content in the concentrate expressed as a mass fraction.

For example, for the untreated copper concentrate leached in 8 wt.% NH_4OH, the ICP-OES concentration measured in the threefold-diluted sample was 9267.9 mg/L. After applying the dilution factor (DF = 3), the copper concentration in the original leach solution was 27,803.7 mg/L, equivalent to 27.8037 g/L. Using a solid-to-liquid ratio of

1:10 (V/m = 0.01 L/g) and a copper mass fraction of (a = 0.4121), the copper extraction efficiency was calculated as follows:

$$R = \frac{27.8037 \cdot 0.01}{0.4121} \times 100\% = 67.47\% \quad (2)$$

Similarly, for the untreated concentrate leached in 15 wt.% citric acid, the measured Cu concentration was 10,603.2 mg/L. After applying the threefold dilution correction, the concentration in the original leach solution was 31.8096 g/L, giving a calculated copper extraction efficiency of 77.18% under the same solid-to-liquid ratio and copper-content assumption.

Since the objective of this work was to investigate copper recovery from the concentrate, the discussion of the leaching results focuses primarily on copper extraction efficiency. All leaching experiments were performed in triplicate under identical experimental conditions. The results are presented as mean values with the corresponding standard deviations (mean ± SD).

2.5. Elemental Analysis of Leaching Solutions Using ICP-OES

The concentrations of the dissolved metals in the leaching solutions were determined by inductively coupled plasma atomic emission spectrometry (ICP-OES). All analyses were carried out with a Thermo Scientific iCAP PRO XP DUO spectrometer (Thermo Fisher Scientific, Bremen, Germany). The concentrations of copper, iron and other dissolved metals were measured quantitatively and the data obtained were used to calculate the metal yields. The results of the chemical analysis also served to evaluate the influence of high-energy milling on the leaching performance of the copper concentrate and to determine the optimal operating parameters for the hydrometallurgical process. For the leaching experiments, three independent experimental replicates were analyzed, and the variability among replicate measurements was expressed as the standard deviation. The concentrations of Cu, Fe, Si, Pb, Mg, and Al in the leach solutions were determined by ICP-OES. These data were used to assess the dissolution behavior of copper relative to the accompanying elements. Before ICP-OES analysis, the leachate samples were diluted threefold. Therefore, the concentrations measured by ICP-OES were corrected using a dilution factor (DF) of 3 to obtain the corresponding concentrations in the original leach solutions. The corrected concentration was calculated as ($C_{corrected} = C_{measured} \times DF$). The dilution correction was applied to all measured elements (Cu, Fe, Si, Pb, Mg, and Al), and the corresponding standard deviations were multiplied by the same factor. The corrected concentrations were used for the calculation of metal extraction efficiencies according to Equation (1).

2.6. Statistical Analysis

All leaching experiments were performed in triplicate, and the results are expressed as mean ± standard deviation (SD). Statistical analyses were conducted to evaluate differences in copper extraction efficiency among the investigated experimental conditions. One-way analysis of variance (ANOVA) was used to evaluate differences among the experimental groups, followed by Tukey's honestly significant difference (HSD) post hoc test for pairwise comparisons, where appropriate. Particular attention was given to comparisons between milling durations of 45 and 60 min, ammonium hydroxide concentrations of 8 and 10 wt.%, and citric acid concentrations of 15 and 20 wt.%. Statistical significance was defined as $p < 0.05$.

3. Results and Discussion

3.1. Structural and Morphological Changes in Copper Concentrate During High-Energy Milling

The influence of high-energy milling on the structural, morphological, particle-size, and accessible surface characteristics of the copper concentrate was evaluated using XRD, SEM, laser diffraction, and BET analysis. These complementary methods were used to identify observable changes in the mineralogical structure and particle morphology of the concentrate after milling. The interpretation presented in this section is based on the complementary evidence obtained from XRD, SEM, BET, and particle-size analysis. The XRD patterns of the untreated copper concentrate and the sample milled for 60 min are presented in Figure 2.

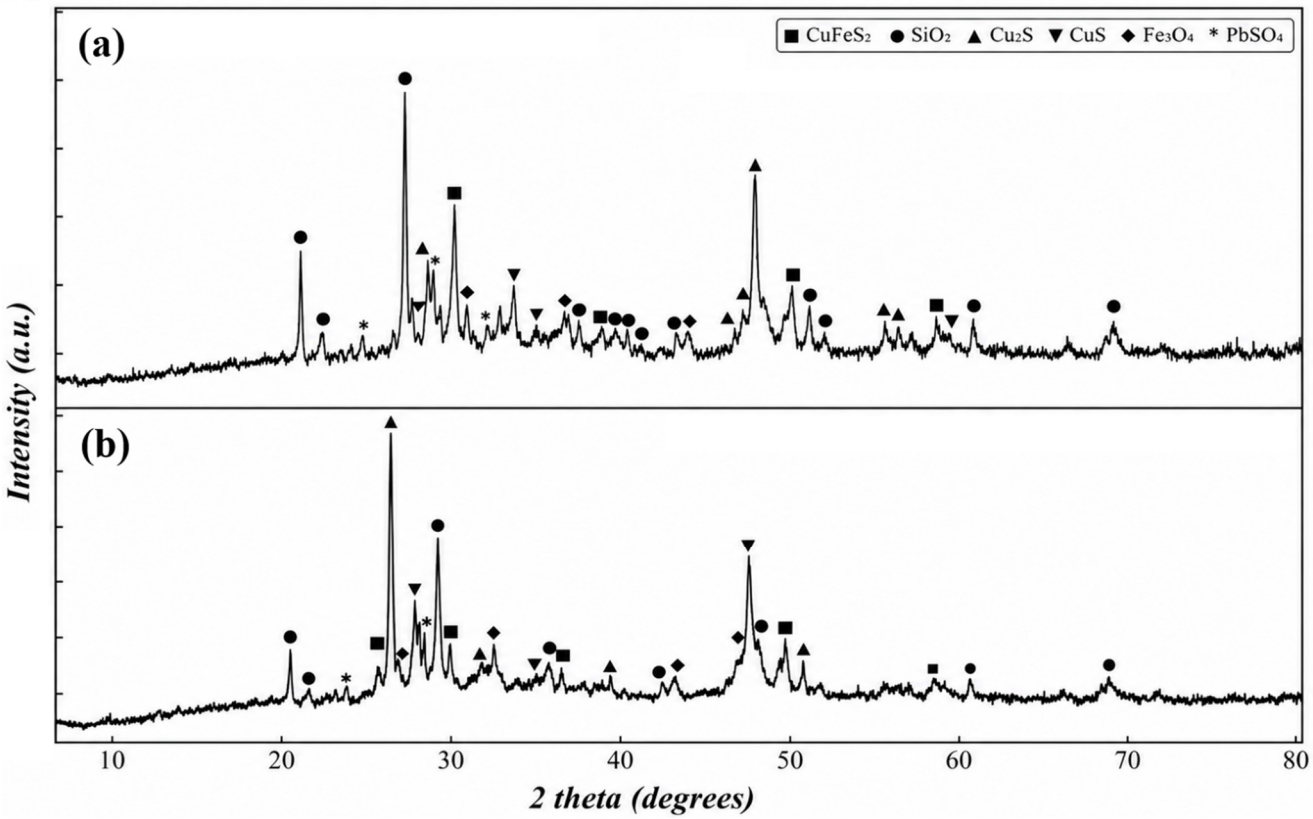


Figure 2. XRD patterns of the initial copper concentrate (**a**) and the sample after 60 min of high-energy milling (**b**).

X-ray diffraction analysis showed that both samples consisted predominantly of chalcopyrite, quartz, copper sulfides, magnetite, and minor amounts of lead sulfate. The principal qualitative observations obtained from the XRD patterns before and after milling are summarized in Table 2.

The characteristic reflections of the principal mineral phases remained detectable after 60 min of milling, indicating that no major qualitative phase transformation occurred under the investigated conditions. Nevertheless, differences in peak shape and relative intensity were observed, particularly in the 27–30° and 47–50° (2θ) regions. These changes are consistent with milling-induced structural modification, including crystallite-size reduction, lattice strain, and increased structural disorder [14–16]. However, the present XRD data do not allow these individual contributions to be quantitatively distinguished. The present XRD data do not, however, allow the individual contributions of crystallite-size reduction, lattice strain, structural disorder, or partial amorphization to be quantitatively distinguished. Therefore, no quantitative conclusions regarding crystallite size, defect density, or degree

of amorphization are drawn from the diffraction patterns. The XRD results are interpreted conservatively as evidence of milling-induced structural modification while the principal mineralogical composition remains detectable. It should also be noted that the milling was performed in ambient air, and therefore possible surface oxidation of sulfide minerals cannot be completely excluded. In addition, stainless-steel milling media may potentially contribute Fe, Cr, or Ni to the milled material. Since the present study did not include dedicated quantitative measurements of these elements before and after milling or direct determination of milling-media mass loss, the contribution of these effects to the observed leaching behavior cannot be quantitatively assessed. Accordingly, the enhanced copper extraction is interpreted primarily as an experimentally observed consequence of high-energy milling, while the individual contributions of surface oxidation and possible media-derived contamination remain unresolved. High-energy milling was conducted in ambient air using a stainless-steel jar and stainless-steel balls. Therefore, possible surface oxidation of sulfide minerals and contamination by Fe, Cr, and Ni from the milling media cannot be completely excluded. Because Fe, Cr, and Ni concentrations before and after milling, as well as milling-media wear or mass loss, were not experimentally quantified in the present study, their individual contributions to the subsequent leaching behavior cannot be quantitatively assessed. Therefore, the possible contribution of media-derived elements is explicitly considered a limitation of the present study, and no mechanistic conclusion is attributed specifically to milling-media contamination.

Table 2. Summary of the Principal XRD Observations Before and After High-Energy Milling.

Diffraction Region (2θ)	Main Phase(s)	Initial Concentrate	Milled Concentrate	Main Observation
27–30°	SiO_2, Cu_2S	Sharp, well-defined diffraction peaks	Broader peaks with reduced relative intensity	Peak broadening and intensity reduction indicate structural modification after milling
47–50°	Cu_2S, CuS	Distinct diffraction peaks	Broader peaks with changes in relative intensity	Structural changes observed while copper sulfide phases remain present
$CuFeS_2$ reflections	Chalcopyrite	Clearly identifiable	Clearly identifiable	No qualitative phase transformation observed
Fe_3O_4 reflections	Magnetite	Present	Present	No significant qualitative change observed
$PbSO_4$ reflections	Lead sulfate	Weak reflections	Weak reflections	Phase remains detectable after high-energy milling
Overall diffraction pattern	—	Sharp diffraction peaks	Broadened peaks with lower relative intensities	High-energy milling affected the structural state of the concentrate without changing its principal mineralogical composition

The morphological evolution of the copper concentrate as a function of milling duration was systematically examined by SEM. Figure 3 presents SEM micrographs of the untreated concentrate and samples milled for 15, 30, 45, and 60 min, obtained at the same magnification of 5000×.

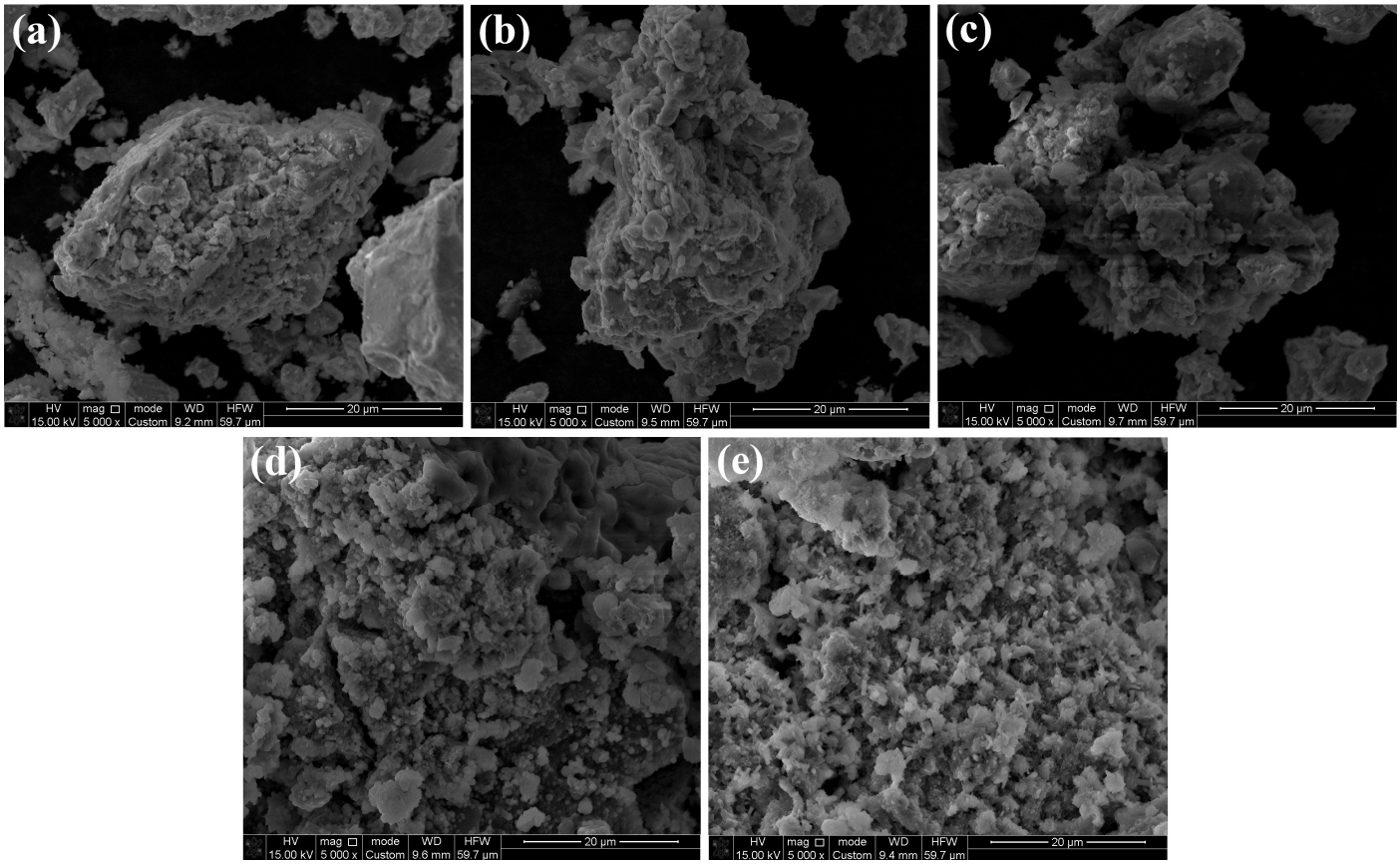


Figure 3. SEM micrographs showing the morphological evolution of the copper concentrate as a function of high-energy milling time: (**a**) untreated (0 min), (**b**) 15 min, (**c**) 30 min, (**d**) 45 min, and (**e**) 60 min. Magnification: 5000×; scale bar: 20 µm.

SEM observations provide direct evidence of the progressive morphological evolution of the copper concentrate during high-energy milling (Figure 3). The untreated sample (Figure 3a) is characterized predominantly by relatively large and compact irregular particles with heterogeneous surfaces. After 15 min of milling (Figure 3b), deformation and disruption of the original particle morphology become evident, although relatively coarse particle assemblies remain present. With increasing milling time to 30 min (Figure 3c), further fragmentation is observed, resulting in a more heterogeneous morphology consisting of smaller irregular fragments associated with residual coarse particles.

More pronounced morphological modification is observed after 45 min (Figure 3d), where numerous fine fragments coexist with larger particle assemblies. After 60 min of milling (Figure 3e), the original compact particle morphology is substantially disrupted, and the sample exhibits a highly heterogeneous structure containing abundant fine irregular fragments. Overall, the SEM observations demonstrate a progressive modification of particle morphology with increasing milling duration, characterized primarily by fragmentation and disruption of the initial coarse particles.

These morphological observations are consistent with the leaching results, which showed higher copper extraction for the milled samples than for the untreated concentrate under the investigated conditions. However, the present data do not allow the improvement in copper extraction to be attributed exclusively to particle fragmentation or changes in surface area, because high-energy milling may simultaneously induce structural modifications, as indicated by the XRD results. Therefore, the SEM and XRD observations are interpreted as complementary evidence of milling-induced morphological and structural changes associated with the observed improvement in leaching performance.

It should be emphasized that the SEM observations provide qualitative morphological evidence and do not constitute quantitative measurements of particle-size distribution or specific surface area. Consequently, although particle fragmentation is clearly observed, the SEM observations alone do not provide quantitative measurements of particle-size distribution or specific surface area. No quantitative conclusions regarding surface-area changes are therefore drawn from the SEM images, and the interpretation is restricted to the morphological features directly observed by SEM.

To quantitatively evaluate the changes in the accessible specific surface area induced by high-energy milling, Brunauer–Emmett–Teller (BET) analysis was performed for the untreated copper concentrate and samples milled for 15, 30, 45, and 60 min. The corresponding nitrogen adsorption–desorption isotherms and BET specific surface area values are presented in Figure 4.

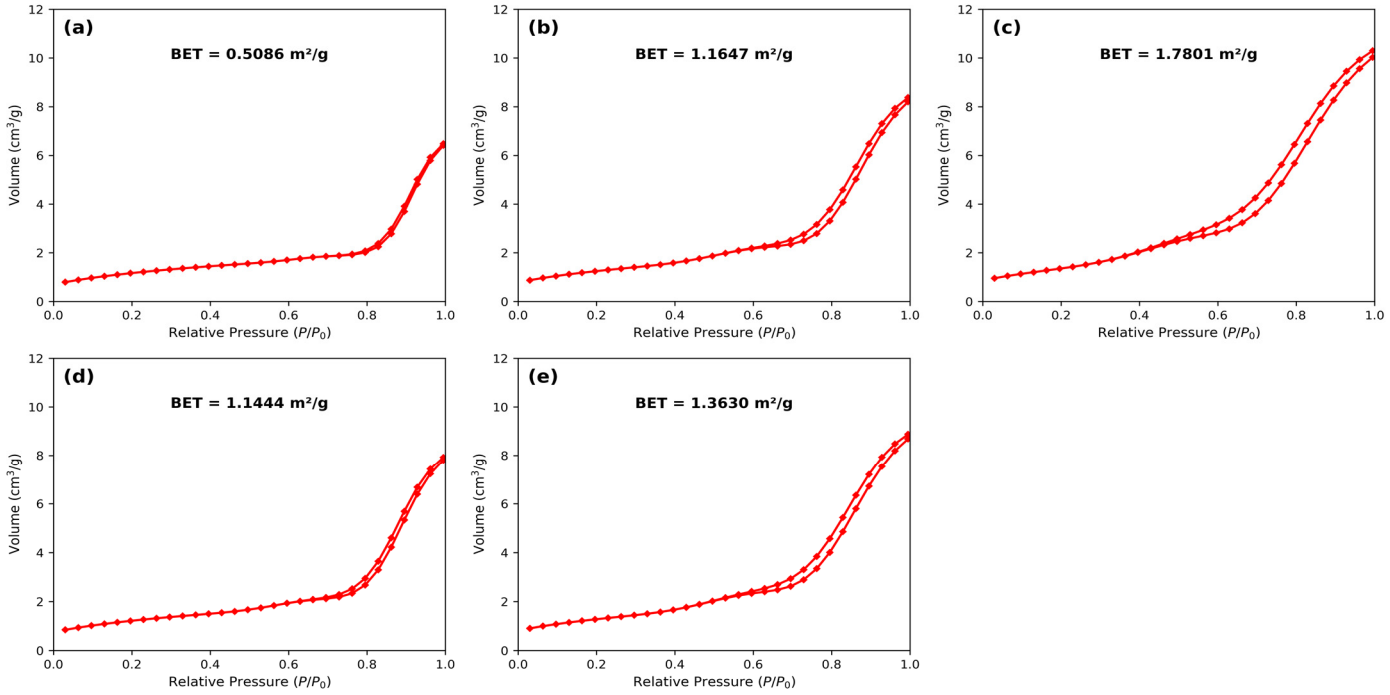


Figure 4. Nitrogen adsorption–desorption isotherms and BET specific surface area of the copper concentrate before and after high-energy milling: (**a**) initial concentrate, (**b**) 15 min, (**c**) 30 min, (**d**) 45 min, and (**e**) 60 min. The adsorption and desorption branches are shown as separate curves.

The initial copper concentrate exhibited a BET specific surface area of 0.5086 m^2/g. After 15 min of milling, the specific surface area increased to 1.1647 m^2/g, corresponding to an approximately 129% increase relative to the untreated concentrate. The maximum BET surface area of 1.7801 m^2/g was obtained after 30 min of milling, representing an approximately 3.5-fold increase compared with the initial sample. With further milling, the BET surface area decreased to 1.1444 m^2/g after 45 min and subsequently increased slightly to 1.3630 m^2/g after 60 min. Thus, the specific surface area did not increase monotonically with milling duration. The maximum value observed at 30 min indicates that the initial stage of high-energy milling was particularly effective in generating new accessible surface area, whereas prolonged milling resulted in a more complex evolution of the accessible surface area. The decrease after 45 min and partial recovery after 60 min indicate that particle-size reduction alone does not fully determine the measured BET surface area. Such behavior may reflect changes in particle packing, surface accessibility, and the development or closure of accessible interparticle or intraparticle voids; however, the present measurements do not allow these individual contributions to be distinguished quantitatively. The BET results

complement the SEM and particle-size distribution analyses. SEM observations showed progressive fragmentation and disruption of the initial coarse particles, while the particle-size analysis demonstrated a pronounced reduction in D50 and D90 during milling. The BET measurements provide additional quantitative evidence that high-energy milling substantially modified the accessible specific surface area of the concentrate. However, the maximum BET surface area was reached after 30 min, whereas the highest copper extraction in ammonium hydroxide and citric acid solutions was obtained after 45 and 60 min of milling, respectively. Therefore, the improvement in copper extraction cannot be attributed solely to an increase in BET surface area. Instead, the leaching enhancement should be considered as the combined result of particle fragmentation, changes in accessible surface area, and milling-induced structural modification observed by XRD.

Particle-size distribution analysis provided quantitative evidence of the particle refinement induced by high-energy milling (Figure 5). The untreated copper concentrate exhibited a broad and heterogeneous particle-size distribution extending toward the coarse-particle range, with D10, D50, and D90 values of 1.078, 5.030, and 57.365 μm, respectively (Table 3). The pronounced coarse-particle fraction is consistent with the relatively large and compact particles observed in the SEM micrograph of the untreated concentrate (Figure 3a). After 15 min of milling, the particle-size distribution shifted markedly toward the fine-particle range. The D50 decreased from 5.030 to 1.417 μm, while D90 decreased from 57.365 to 4.809 μm. The average particle size (Dav) simultaneously decreased from 22.792 to 2.234 μm. These changes demonstrate that the most pronounced particle refinement occurred during the initial stage of high-energy milling and are consistent with the fragmentation observed by SEM. Further milling to 30 min resulted in a relatively small additional change in the characteristic particle-size parameters. The minimum D50 value of 1.193 μm and a Dav of 2.220 μm were obtained at this milling duration. At 45 min, D50 remained low at 1.234 μm, while D90 was 5.128 μm. After 60 min, a slight increase in D50 and Dav to 1.335 and 2.452 μm, respectively, was observed, whereas D90 remained at a relatively low value of 5.215 μm. These results indicate that the major reduction in particle size occurred during the first 15–30 min of milling, while prolonged milling produced comparatively smaller changes in the characteristic particle-size parameters.

The distribution span also decreased substantially from 11.190 for the untreated concentrate to 2.921 after 15 min of milling, followed by values of 3.775, 3.568, and 3.362 after 30, 45, and 60 min, respectively (Table 3). Thus, high-energy milling not only reduced the characteristic particle size but also substantially narrowed the particle-size distribution relative to the untreated concentrate. Overall, the PSD results quantitatively confirm the particle fragmentation observed by SEM and demonstrate that the principal particle-size refinement occurred during the early stage of milling. From a technological perspective, the use of a planetary ball mill at 500 rpm and a ball-to-powder ratio of 20:1 provides effective laboratory-scale activation of the copper concentrate; however, the present study did not include direct measurement of electrical energy consumption. Therefore, the specific energy requirement (e.g., kWh kg^{-1}) cannot be quantitatively reported or directly compared with industrial milling technologies. In addition, scale-up from laboratory planetary milling to an industrial process would require consideration of mill capacity, energy efficiency, throughput, residence time, and media consumption. The present results should therefore be regarded as a laboratory-scale demonstration of the effect of milling duration on subsequent copper leaching rather than as a complete techno-economic assessment of industrial implementation.

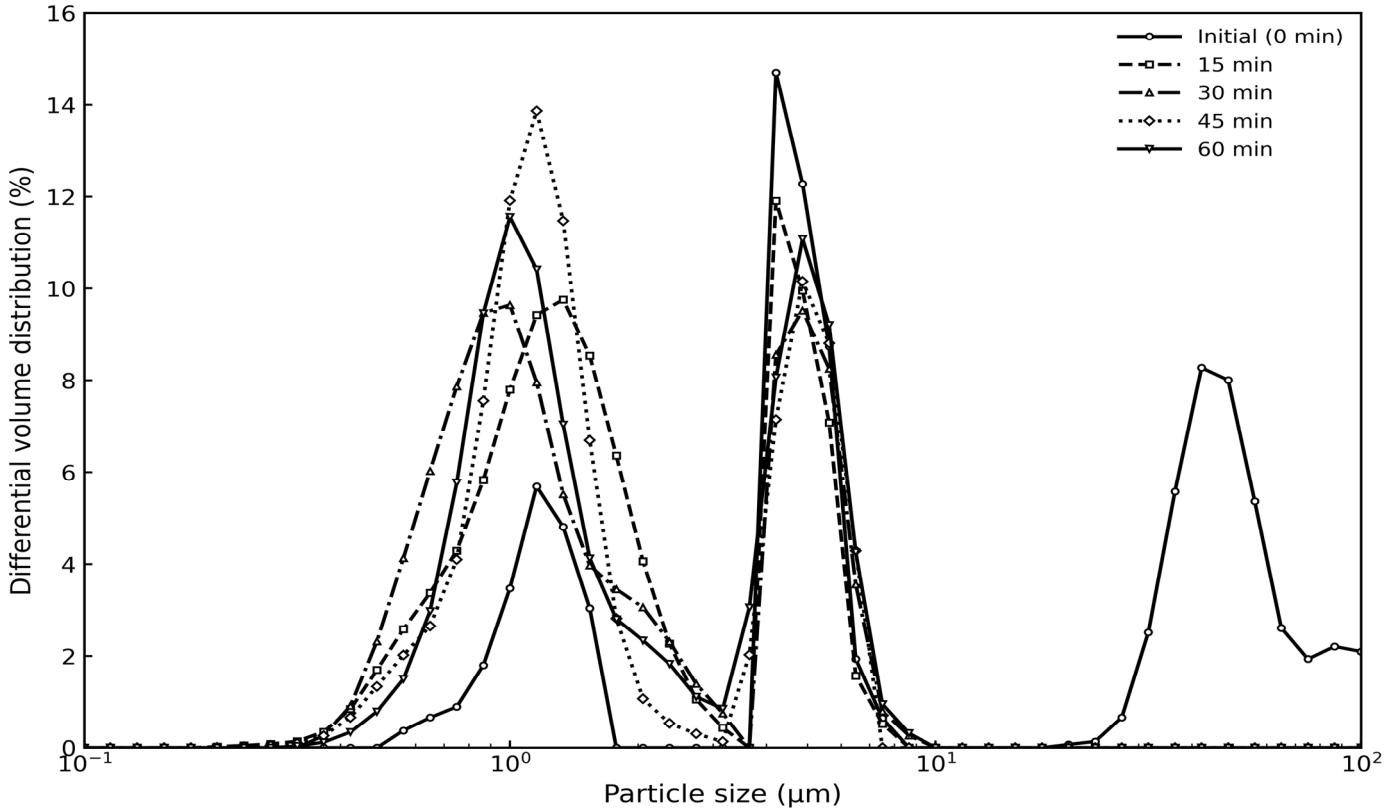


Figure 5. Particle-size distributions of the copper concentrate before and after high-energy milling determined by laser diffraction.

Table 3. Particle-size characteristics of the copper concentrate before and after high-energy milling determined by laser diffraction.

Powder	D10 (µm)	D50 (µm)	D90 (µm)	Dav (µm)	Span
Intial Cu concentrate	1.078	5.030	57.365	22.792	11.190
15 min MT	0.670	1.417	4.809	2.234	2.921
30 min MT	0.598	1.193	5.101	2.220	3.775
45 min MT	0.725	1.234	5.128	2.245	3.568
60 min MT	0.727	1.335	5.215	2.452	3.362

3.2. Effect of Leaching Parameters on Metal Extraction Efficiency

The leaching performance was evaluated primarily based on copper extraction because the main objective of this study was to investigate copper recovery from the concentrate. In addition, the concentrations of the major accompanying elements in the leach solutions were determined by ICP-OES to evaluate their dissolution behavior relative to copper. The extraction efficiency of metals during leaching strongly depends on the selected process conditions. Operating parameters such as reagent concentration, temperature, leaching time, and the solid–liquid ratio play a decisive role in the dissolution behavior of the mineral phases and the yield of valuable metals. Therefore, determining optimal leaching conditions is essential to maximize the performance of hydrometallurgical processes [17]. In the present study, copper leaching with citric acid and ammonia solution was carried out, and the effects of the most important operating parameters were systematically investigated. The reaction of copper extraction to changes in individual variables was analyzed to determine the conditions with the highest yield. Particular attention was paid to the leaching temperature

and the reaction time, as these parameters directly influence mineral dissolution rates, mass transport characteristics, and overall leaching performance. The relationship between temperature, leaching time and copper extraction efficiency is shown in Figure 6.

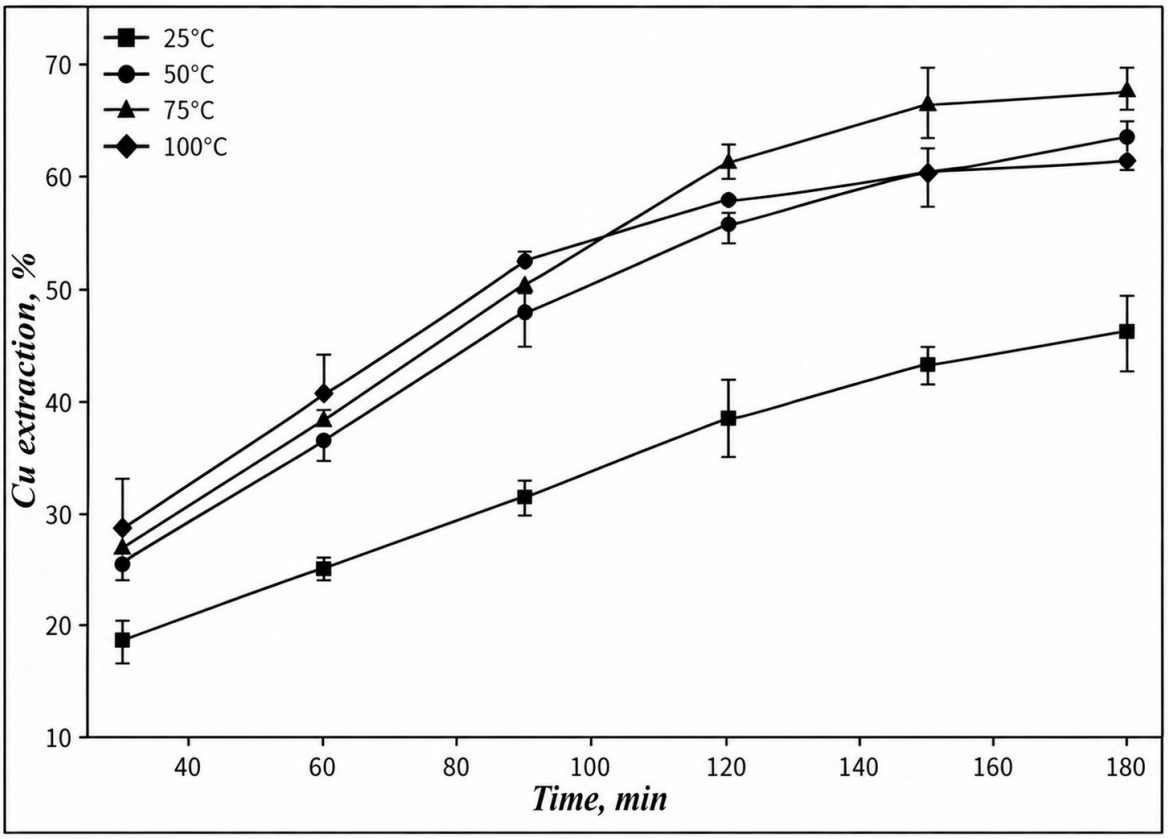


Figure 6. Effect of leaching temperature and time on copper extraction efficiency in 8 wt.% NH_4OH solution. Fixed experimental conditions: untreated copper concentrate, solid-to-liquid ratio = 1:10, stirring speed = 500 rpm. Data are presented as mean ± SD (n = 3).

Figure 6 illustrates the influence of leaching temperature and reaction time on copper yield in an ammoniacal medium. The results show that the copper yield increased steadily with increasing leaching time at all investigated temperatures. This behavior can be attributed to improved mass transfer between the solid and liquid phases, as well as extended contact time between the mineral particles and the leaching solution, which promotes the dissolution of copper-containing phases. During the first 30 min of leaching, the copper yield remained relatively low at all the temperatures investigated. An increase in temperature accelerated the initial rate of copper dissolution, due to enhanced diffusion processes and more intensive formation of ammonia-copper complexes. The increased temperature promotes both mass transfer and interaction between the leaching reagent and the copper-containing mineral phases, thus facilitating metal dissolution. With a leaching time of 90 min, a significant improvement in the copper yield was observed under all experimental conditions. In this phase, copper yields of 50% and 52% were achieved at 75 °C and 100 °C, respectively. In an alkaline ammonia medium, the dissolved copper ions readily coordinate with ammonia molecules and form the stable tetraammine-copper(II) complex. This increases the stability of the copper in solution and promotes its continuous dissolution during the leaching process [18]:

$$Cu^{2+} + 4NH_3 \rightarrow [Cu(NH_3)_4]^{2+} \quad (3)$$

Although copper may occur in different oxidation states within sulfide minerals, the oxidation state of dissolved copper was not determined in the present study. The leaching experiments were conducted in contact with atmospheric air, and dissolved oxygen may therefore have contributed to oxidation reactions at the mineral–solution interface. However, this contribution cannot be quantified because dissolved oxygen concentration and redox potential were not measured. Iron-bearing phases identified in the concentrate, including magnetite and iron-containing sulfide minerals, may also be relevant to the redox chemistry of the leaching system. If Fe(III) species were generated or present in solution, they could potentially contribute to the oxidative dissolution of copper sulfides. Nevertheless, the presence and concentration of dissolved Fe(III) were not determined, and the ICP-OES measurements of total dissolved iron do not establish its oxidation state. Therefore, an Fe(III)-mediated oxidation pathway cannot be confirmed from the available experimental data. Accordingly, the enhanced copper extraction observed after high-energy milling is interpreted in terms of the experimentally observed changes in particle size, morphology, accessible surface area, and structural state, together with the chemical interactions occurring during leaching. The relative contributions of atmospheric oxygen, iron-mediated oxidation, and other possible pathways remain unresolved. No specific oxidation mechanism is claimed without direct redox measurements and oxidation-state-specific analysis. In addition, high-energy milling was conducted under ambient air, which may have modified the surface state and reactivity of the mineral particles prior to leaching. Therefore, the relatively high copper extraction observed after milling is not attributed to a single oxidation mechanism, but rather to the combined effects of milling-induced structural modification, particle fragmentation, increased accessibility of copper-bearing phases, mass transfer, and chemical interactions between the mineral phases and the leaching reagents. After 120 min of leaching, the influence of temperature became more noticeable. The copper extraction reached 61% at 75 °C, compared with 58% at 100 °C. Considering the experimental variability indicated by the error bars, the difference between these two conditions was relatively small. Therefore, the higher extraction observed at 75 °C should not be interpreted as statistically significant without further statistical testing. A further increase in temperature did not result in a proportional improvement in copper extraction. This behavior may be related to the increased volatility of ammonia at higher temperatures, which can decrease the concentration of free NH_3 available for complex formation in the leaching solution. After 180 min of leaching, the highest observed mean copper extraction of 67% was obtained at 75 °C. At 100 °C, a slight decrease in copper extraction was observed. This decrease may be associated with intensive ammonia evaporation and the resulting depletion of the complexing agent, which may adversely affect the stability of dissolved copper complexes and the overall leaching performance. Overall, the results indicate that temperature and leaching time influenced copper extraction under the investigated conditions. Therefore, 75 °C and 180 min were selected as the most favorable conditions within the investigated experimental range based on the highest observed mean copper extraction. These results also indicate that increasing the temperature beyond the optimum value does not necessarily improve the performance of ammoniacal leaching systems and underline the importance of choosing suitable technological conditions to maximize metal yield.

In the hydrometallurgical treatment of copper concentrates, the concentration of the leaching reagent plays a decisive role in the degree of metal dissolution and extraction efficiency. Therefore, the effects of the NH_4OH and citric acid concentrations on the copper yield were systematically investigated. The reagent concentrations were varied under controlled experimental conditions, and the corresponding changes in copper yield were evaluated to determine the relationship between reagent concentration and leaching performance.

As shown in Figure 7a, increasing the NH_4OH concentration from 5% to 8% increased the mean copper extraction from approximately 48% to 66%. At 10% NH_4OH, the mean extraction decreased to approximately 60%. The 8 wt.% NH_4OH condition yielded the highest observed mean copper extraction within the investigated concentration range. However, the difference between 8 and 10 wt.% NH_4OH was not statistically significant ($p = 0.077$). Therefore, 8 wt.% NH_4OH provided the highest observed mean extraction, but its superiority over 10 wt.% NH_4OH was not statistically established. This improvement can be attributed to the increased ability of ammonia to form stable coordination complexes with copper ions, thereby promoting their dissolution and stabilization in the leaching solution. The decrease observed at 10 wt.% NH_4OH may be related to changes in mass-transfer conditions and the approach of the leaching system toward equilibrium. As shown in Figure 7b, an increase in the citric acid concentration had a positive effect on the copper extraction. An increase in the citric acid concentration from 2.5% to 15% increased the copper extraction from 45% to 77%. This improvement is attributed to the ability of organic acids to effectively dissolve mineral phases and facilitate the transition of copper ions into solution. In the leaching system, copper ions react with citric acid and form the following coordination complex [19]:

$$Cu^{2+} + C_6H_5O_7{}^{3-} \rightarrow [Cu(C_6H_5O_7)]^- \quad (4)$$

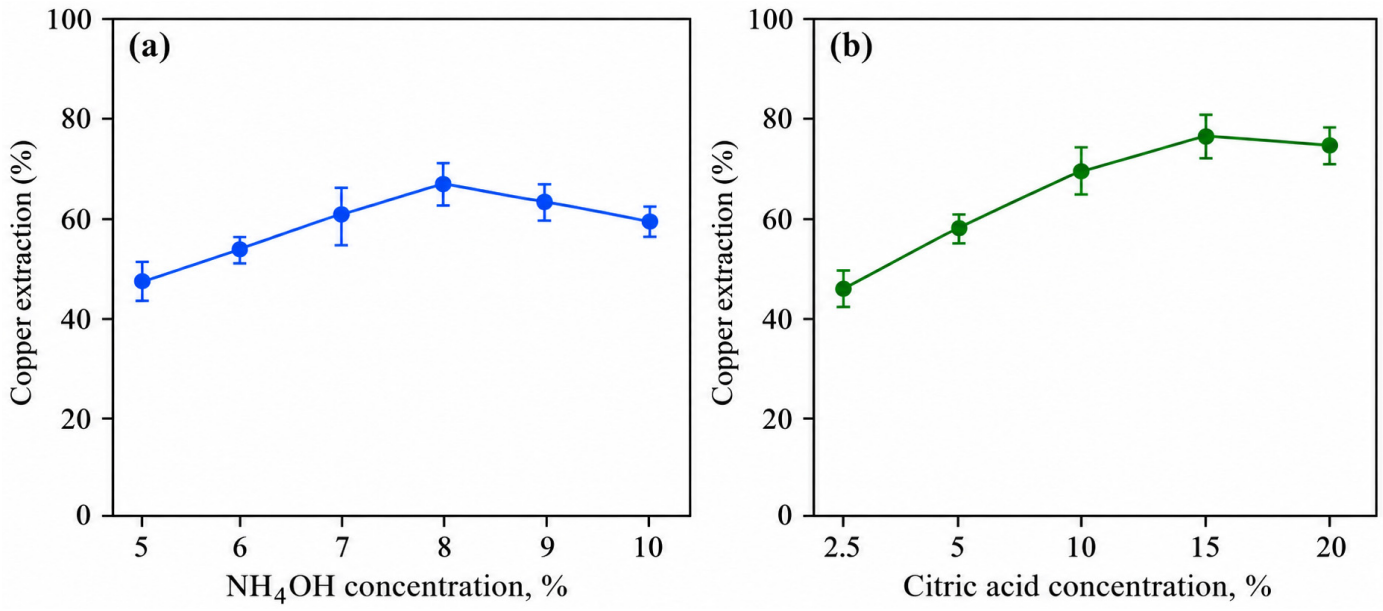


Figure 7. Effect of (**a**) NH_4OH and (**b**) citric acid concentrations on copper extraction efficiency. Fixed experimental conditions: untreated copper concentrate, leaching temperature = 75 °C, leaching time = 180 min, solid-to-liquid ratio = 1:10, and stirring speed = 500 rpm. Data are presented as mean ± SD ($n = 3$). Pairwise comparisons: 8 versus 10 wt.% NH_4OH, $p = 0.077$; 15 versus 20 wt.% citric acid, $p = 0.748$. ns, not statistically significant ($p \geq 0.05$).

During citric acid leaching, dissolved copper ions can interact with citrate species to form soluble copper–citrate complexes, which may contribute to maintaining copper in the liquid phase [19]. Increasing the citric acid concentration to 20 wt.% did not result in a further improvement in copper extraction, which remained at approximately 76%. Considering the experimental variability indicated by the error bars, the difference between 15 and 20 wt.% citric acid was relatively small. The slight decrease at 20 wt.% should therefore be interpreted cautiously and may reflect experimental variability and changes in the leaching equilibrium at higher citrate concentrations. Therefore, 15 wt.% citric acid gave the highest observed copper extraction within the investigated range. In comparison,

the highest extraction obtained with ammonium hydroxide was 66% at 8 wt.% NH_4OH. For ammonium hydroxide leaching, the difference in copper extraction between 8 and 10 wt.% NH_4OH was not statistically significant ($p = 0.077$). Similarly, the difference between 15 and 20 wt.% citric acid was not statistically significant ($p = 0.748$). Therefore, these concentrations yielded the highest observed mean extraction values within the investigated ranges, but their superiority over the adjacent concentrations was not statistically established. Under the investigated conditions, citric acid provided higher copper extraction than ammonium hydroxide. Overall, the leaching experiments showed that copper extraction was influenced by reagent concentration, temperature, and leaching time. Under the investigated conditions, the highest copper extraction in ammonium hydroxide solution was obtained at 75 °C after 180 min, while an NH_4OH concentration of 8 wt.% provided the highest extraction within the investigated concentration range. In citric acid solution, the highest copper extraction was obtained at a concentration of 15 wt.%. These conditions were subsequently selected for evaluating the influence of high-energy milling on copper extraction, as discussed separately in Section 3.4.

3.3. Phase and Morphological Characteristics of Solid Residues After Leaching

Characterization of the solid residue after leaching provides additional information on the mineral phases that remained under the investigated conditions. The phase composition and morphology of the solid residue obtained after citric acid leaching were examined by XRD and SEM, respectively, and the results are presented in Figure 8.

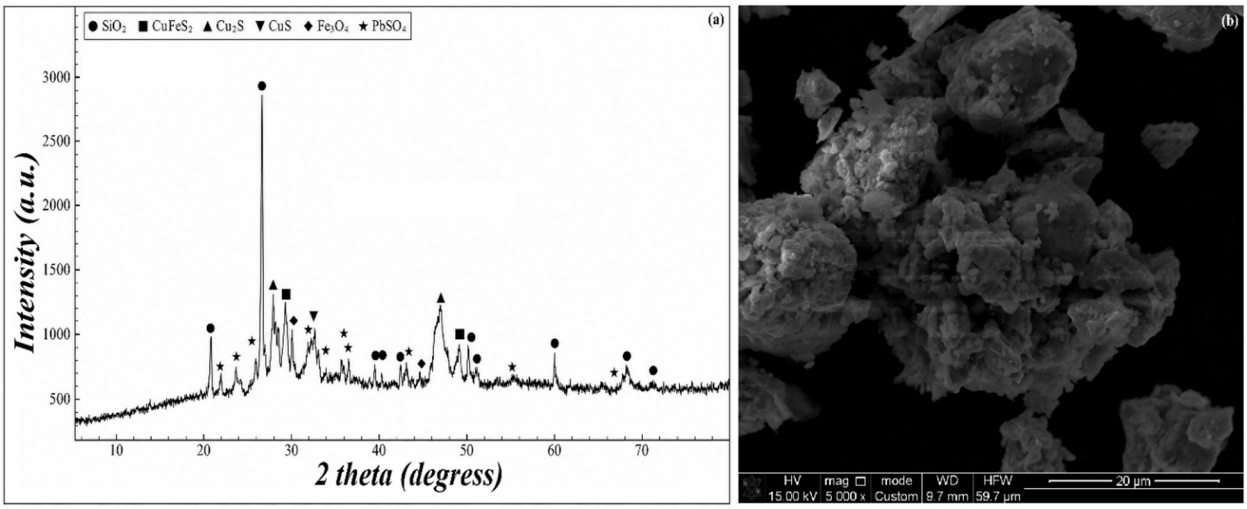


Figure 8. XRD pattern (**a**) and SEM micrograph (**b**) of the copper concentrate residue after citric acid leaching.

The XRD pattern of the leaching residue shows that quartz, chalcopyrite, chalcocite, covellite, magnetite, and lead sulfate remained detectable after leaching. The XRD pattern of the initial concentrate did not reveal distinct secondary copper oxide phases among the identifiable crystalline phases. Similarly, no distinct secondary copper oxide phases were identified in the XRD pattern of the solid residue obtained after citric acid leaching. The detected crystalline copper-bearing phases were predominantly sulfides, including chalcopyrite, chalcocite, and covellite. These observations indicate that secondary copper oxide minerals were not identified as major crystalline phases in the analyzed samples. However, the available XRD data do not exclude the possible presence of minor, poorly crystalline, or amorphous copper-containing phases below the detection capability of the method. Therefore, the oxygen content detected by SEM–EDS cannot be used independently to establish the presence or abundance of secondary copper oxide minerals. The persistence

of copper sulfide phases in the residue is consistent with incomplete dissolution under the investigated conditions, although quantitative phase analysis would be required to determine the dissolution extent of individual minerals. Compared with the initial concentrate, reduced relative intensities were observed for several reflections associated with copper-bearing sulfide phases. These changes are consistent with partial dissolution of copper-bearing phases during leaching and with the experimentally measured transfer of copper into the liquid phase. The persistence of chalcopyrite, chalcocite, and covellite in the leaching residue is consistent with incomplete dissolution of these copper sulfide phases under the investigated conditions. However, because quantitative phase analysis was not performed, the extent of dissolution of individual mineral phases cannot be determined directly from the relative diffraction intensities. Quartz remained clearly detectable in the solid residue, while magnetite and lead sulfate reflections were also retained. Their persistence indicates that these phases were not completely dissolved under the investigated leaching conditions. No quantitative conclusions regarding their individual dissolution degrees are therefore drawn from the XRD data. The SEM micrograph of the leaching residue (Figure 8b) shows a heterogeneous morphology with irregular particle surfaces and locally roughened regions. These morphological features differ from those observed for the untreated concentrate and are consistent with modification of the particle surfaces during leaching. However, SEM provides qualitative morphological information only, and the observed surface features cannot by themselves be used to quantify the extent of mineral dissolution. Overall, the XRD and SEM observations of the solid residue are consistent with partial dissolution of copper-bearing phases during citric acid leaching, while quartz, magnetite, lead sulfate, and residual copper-bearing sulfide phases remained detectable. These observations complement the quantitative copper extraction results obtained from analysis of the leaching solution.

3.4. Influence of High-Energy Milling on Copper Extraction

The influence of high-energy milling duration on copper extraction in ammonium hydroxide and citric acid solutions is presented in Figure 9. The experiments were conducted under fixed leaching conditions using 8 wt.% NH_4OH and 15 wt.% citric acid solutions at 75 °C for 180 min, with a solid-to-liquid ratio of 1:10 and a stirring speed of 500 rpm.

In both leaching media, the milled samples exhibited higher copper extraction than the untreated concentrate. In the ammonium hydroxide system, copper extraction increased from 67% for the untreated concentrate to approximately 73% after 15 min and 78% after 30 min of milling. The highest observed mean copper extraction in NH_4OH was obtained after 45 min of milling (approximately 81%), followed by approximately 79% after 60 min. Considering the experimental variability, the difference between these two milling durations was relatively small. Although the highest observed mean copper extraction in the NH_4OH system was obtained after 45 min of milling, the difference between 45 and 60 min was not statistically significant ($p = 0.062$). Therefore, 45 min is identified as the condition yielding the highest observed mean extraction within the investigated range, but its superiority over 60 min was not statistically established.

In the citric acid system, the highest observed mean copper extraction was obtained after 60 min of milling. However, the difference between 45 and 60 min was not statistically significant ($p = 0.748$). Thus, 60 min yielded the highest observed mean extraction within the investigated range, but a statistically significant improvement over 45 min was not demonstrated. The systematic SEM observations presented in Figure 3 show that these changes in leaching behavior occurred concurrently with progressive modification of particle morphology. Increasing milling duration resulted in disruption of the initial compact particles and an increasing occurrence of fine irregular fragments. XRD analysis additionally

revealed changes in diffraction peak shape and relative intensity while the principal mineral phases remained detectable. Taken together, these results demonstrate that high-energy milling modified both the morphology and structural state of the concentrate. The improvement in copper extraction after milling is therefore associated with the experimentally observed morphological and structural modifications. The PSD and BET results provide further quantitative evidence for the physical changes induced by milling. The PSD results indicate that substantial particle fragmentation occurred during the early stage of milling, while the BET specific surface area reached its maximum value of 1.7801 m^2/g after 30 min. However, the highest copper extraction was achieved after 45 min in ammonium hydroxide and after 60 min in citric acid, despite the fact that the maximum BET surface area was observed at 30 min. This difference indicates that the enhanced leaching performance cannot be explained solely by particle-size reduction or an increase in BET surface area. Rather, the results suggest that prolonged milling modifies the physical accessibility and structural state of the concentrate in addition to reducing particle size. Because the individual contributions of particle fragmentation, accessible surface area, and structural modification cannot be quantitatively separated under the present experimental conditions, these factors are considered collectively in interpreting the enhanced copper extraction. However, the present results do not establish a direct causal relationship between any individual physical modification and the increase in copper extraction. Consequently, the relative contributions of particle fragmentation, changes in specific surface area, and milling-induced structural modification cannot be separated quantitatively. The slight decrease in copper extraction in the ammonium hydroxide system between 45 and 60 min should also be interpreted cautiously. Although SEM shows continued morphological modification with increasing milling duration, the available characterization does not provide sufficient evidence to attribute this decrease to particle agglomeration, changes in specific surface area, or another specific mechanism. However, the present measurements do not provide sufficient evidence to identify the specific origin of this decrease. Further targeted experiments would be required to distinguish the individual contributions of particle morphology, surface accessibility, and structural changes to this behavior. Overall, the experimental results demonstrate that high-energy milling is associated with improved copper extraction in both investigated leaching media, although the optimum milling duration depends on the leaching system. Under the investigated conditions, 45 min provided the highest copper extraction in ammonium hydroxide solution, whereas 60 min provided the highest extraction in citric acid solution. The present experimental results do not allow identification of the rate-limiting step of the leaching process, as a dedicated kinetic analysis was not performed. To further assess the dissolution behavior of copper relative to the accompanying elements, the concentrations of Cu, Fe, Si, Pb, Mg, and Al in the leach solutions were determined by ICP-OES. The analyses were performed for samples leached under the selected conditions of 8 wt.% NH_4OH and 15 wt.% citric acid at different high-energy milling durations. The resulting concentrations of dissolved metals are summarized in Table 4.

As shown in Table 4, Cu was the predominant dissolved metal in both leaching systems under the selected conditions. The concentrations of Fe, Si, Pb, Mg, and Al were substantially lower than that of Cu. Increasing the high-energy milling time generally increased the concentrations of the accompanying elements in the leach solutions, although the magnitude of the increase varied depending on the element and leaching medium.

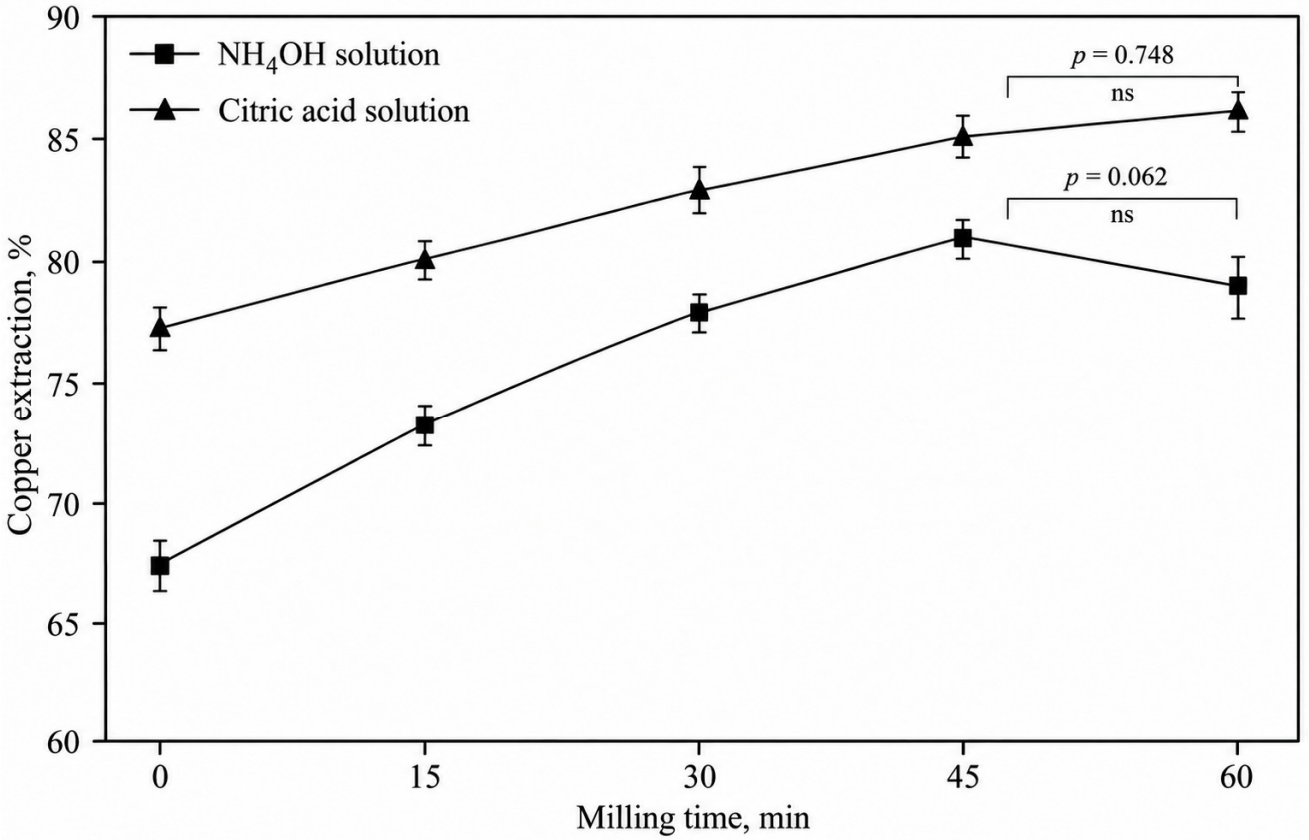


Figure 9. Effect of high-energy milling time on copper extraction from the copper concentrate during leaching in 8 wt.% NH_4OH and 15 wt.% citric acid solutions. ■ NH_4OH solution; ▲ citric acid solution. Fixed experimental conditions: particle size < 100 µm, leaching temperature = 75 °C, leaching time = 180 min, solid-to-liquid ratio = 1:10, and stirring speed = 500 rpm. Data are presented as mean ± SD ($n = 3$). Pairwise comparisons between 45 and 60 min of milling: NH_4OH, $p = 0.062$; citric acid, $p = 0.748$. ns, not statistically significant ($p \geq 0.05$).

Table 4. ICP-OES concentrations of dissolved metals in the original leach solutions obtained using 8 wt.% NH_4OH and 15 wt.% citric acid as a function of high-energy milling time. All concentrations were corrected for a threefold sample dilution and are presented as mean ± SD ($n = 3$).

Leaching Solution	High-Energy Milling Time (min)	Cu (mg/L)	Fe (mg/L)	Si (mg/L)	Pb (mg/L)	Mg (mg/L)	Al (mg/L)
NH_4OH	0	27,803.7 ± 135.6	729.9 ± 14.8	211.2 ± 6.3	96.3 ± 3.9	38.7 ± 1.8	192.6 ± 7.8
	15	30,166.5 ± 157.8	853.5 ± 16.8	277.5 ± 8.4	137.4 ± 5.4	58.5 ± 2.7	289.5 ± 9.9
	30	32,144.7 ± 175.2	1004.1 ± 20.1	395.4 ± 11.7	215.7 ± 8.1	71.1 ± 3.9	398.4 ± 12.6
	45	33,381.0 ± 183.9	1104.3 ± 21.9	566.1 ± 16.2	286.5 ± 10.8	94.8 ± 4.5	487.5 ± 17.7
	60	32,556.6 ± 173.7	1254.9 ± 24.6	614.7 ± 17.7	335.4 ± 12.6	108.0 ± 5.1	581.1 ± 19.8
Citric acid	0	31,809.6 ± 164.1	986.1 ± 18.6	103.8 ± 4.2	362.4 ± 14.1	108.3 ± 5.4	585.9 ± 23.4
	15	33,049.5 ± 172.5	1233.9 ± 24.9	156.3 ± 5.1	480.9 ± 18.9	144.3 ± 8.7	776.7 ± 27.6
	30	34,243.2 ± 179.4	1554.6 ± 32.1	207.9 ± 7.8	534.6 ± 20.1	190.2 ± 8.7	968.1 ± 32.1
	45	35,067.6 ± 184.5	1724.1 ± 34.2	259.8 ± 8.1	635.1 ± 22.2	225.6 ± 9.9	1162.2 ± 39.3
	60	35,520.9 ± 186.3	1998.9 ± 46.8	337.2 ± 11.7	722.7 ± 26.4	260.7 ± 11.1	1370.1 ± 46.2

Note: Concentrations are corrected for the experimentally verified dilution factor of 3 and are reported as mean ± SD ($n = 3$).

4. Conclusions

This study investigated the influence of high-energy milling on the physicochemical characteristics and subsequent hydrometallurgical recovery of copper from an industrial copper concentrate obtained from the Balkhash copper smelter. High-energy milling substantially modified the structural and morphological characteristics of the concentrate, while the principal mineral phases remained detectable. Particle-size analysis confirmed pronounced particle refinement, whereas BET analysis showed a non-monotonic change in accessible surface area with increasing milling time. Under the investigated leaching conditions, the untreated concentrate exhibited maximum copper extraction of 67% in ammonium hydroxide and 77% in citric acid. Milling further enhanced copper extraction, with the highest observed mean values reaching approximately 81% after 45 min in ammonium hydroxide and 86% after 60 min in citric acid. However, the differences between 45 and 60 min of milling were not statistically significant in either leaching system ($p = 0.062$ for NH_4OH and $p = 0.748$ for citric acid). Therefore, these milling durations yielded the highest observed mean extraction values within the investigated range, but their superiority over the adjacent milling duration was not statistically established. ICP-OES analysis showed that Cu was the predominant dissolved metal, while Fe, Si, Pb, Mg, and Al occurred at substantially lower concentrations. The different milling times corresponding to the maximum BET surface area and copper extraction indicate that the improvement in leaching performance cannot be attributed solely to surface-area enlargement or particle-size reduction. Overall, the results demonstrate that high-energy milling is an effective pretreatment for enhancing copper extraction from the investigated Balkhash copper concentrate, although the individual contributions of particle fragmentation, surface-area changes, structural modification, and other possible effects cannot be quantitatively separated under the present experimental conditions.

Author Contributions: Conceptualization, K.K.; methodology, A.N.B., A.S.A., and L.A.M.; investigation, A.S.A., M.T.Y., and A.N.B.; resources, K.K.; writing—original draft preparation, K.K., L.A.M.; writing—review and editing, K.K.; visualization, A.S.A., A.N.B., M.T.Y., and L.A.M.; funding acquisition, K.K.; All authors have read and agreed to the published version of the manuscript.

Funding: This research was funded by the Science Committee of the Ministry of Science and Higher Education of the Republic of Kazakhstan (Grant no. BR28713557).

Data Availability Statement: The original contributions presented in this study are included in the article. Further inquiries can be directed to the corresponding author.

Conflicts of Interest: The authors declare no conflicts of interest.

References

1. Cheje Machaca, D.M.; Botelho, A.B., Jr.; de Carvalho, T.C.; Tenório, J.A.S.; Espinosa, D.C.R. Hydrometallurgical processing of chalcopyrite: A review of leaching techniques. *Int. J. Miner. Metall. Mater.* **2024**, *31*, 2537–2555. [CrossRef]
2. Ji, G.; Liao, Y.; Wu, Y.; Xi, J.; Liu, Q. A review on the research of hydrometallurgical leaching of low-grade complex chalcopyrite. *J. Sustain Metall.* **2022**, *8*, 964–977. [CrossRef]
3. Dakkoune, A.; Bourgeois, F.; Po, A.; Joulian, C.; Hubau, A.; Touzé, S.; Julcour, C.; Guezennec, A.G.; Cassayre, L. Hydrometallurgical processing of chalcopyrite by attrition-aided leaching. *ACS Eng. Au* **2023**, *3*, 195–209. [CrossRef]
4. Jiang, L.; Leng, H.; Han, B. Dissolution and passivation mechanism of chalcopyrite during pressurized water leaching. *Minerals* **2023**, *13*, 996. [CrossRef]
5. Akhgar, B.N.; Kavanlouei, M.; Farhoudi, S.; Rohzad, M.H. Impact of mechanical activation and mechanochemical activation on microstructural changes, leaching rate and leachability of natural chalcopyrite. *Miner. Eng.* **2024**, *217*, 108962. [CrossRef]
6. Li, Y.; Tian, Z.; Wang, X.; Yang, C. Effect of Mechanical Activation on Electrochemical Properties of Chalcopyrite in Iron-Containing Sulfuric Acid Solutions. *Metals* **2025**, *15*, 1075. [CrossRef]
7. Barton, I.F.; Hiskey, J.B. Chemical, crystallographic, and electromagnetic variability in natural chalcopyrite and implications for leaching. *Miner. Eng.* **2022**, *189*, 107867. [CrossRef]

8. Cao, S.T.; Zheng, X.F.; Nie, Z.Y.; Zhou, Y.H.; Liu, H.C.; Chen, J.H.; Yang, H.Y.; Xia, J.L. Mechanical activation on bioleaching of chalcopyrite: A new insight. *Minerals* **2020**, *10*, 788. [CrossRef]
9. Granata, G.; Takahashi, K.; Kato, T.; Tokoro, C. Mechanochemical activation of chalcopyrite: Relationship between activation mechanism and leaching enhancement. *Miner. Eng.* **2019**, *131*, 280–285. [CrossRef]
10. Bai, Y.; Wang, W.; Zhao, S.; Lu, D.; Xie, F.; Dreisinger, D. Effect of mechanical activation on leaching behavior and mechanism of chalcopyrite. *Mineral. Process. Extr. Metall. Rev.* **2022**, *43*, 440–452. [CrossRef]
11. Kenzhaliyev, B.; Ketegenov, T.; Kamunurm, K.; Batkal, A.; Nadirov, R. Efficient Copper Recovery from Chalcopyrite Using an «Isopropanol–Sulfuric Acid–Sodium Dodecyl Sulfate» System. *Minerals* **2023**, *13*, 1346. [CrossRef]
12. Mussapyrova, L.; Nadirov, R.; Baláž, P.; Rajňák, M.; Bureš, R.; Baláž, M. Selective room-temperature leaching of copper from mechanically activated copper smelter slag. *J. Mater. Res. Technol.* **2021**, *12*, 2011–2025. [CrossRef]
13. Koizhanova, A.K.; Kenzhaliyev, B.K.; Magomedov, D.R.; Erdenova, M.B.; Bakrayeva, A.N.; Abdyldaev, N.N. Hydrometallurgical studies on the leaching of copper from man-made mineral formations. *Kompleks. Ispolz. Miner. Syra Complex Use Miner. Resour.* **2024**, *330*, 32–42. [CrossRef]
14. Baláž, P.; Achimovičová, M.; Baláž, M.; Billik, P.; Cherkezova-Zheleva, Z.; Criado, J.M.; Delogu, F.; Dutková, E.; Gaffet, E.; Gotor, F.J.; et al. Hallmarks of mechanochemistry: From nanoparticles to technology. *Chem. Soc. Rev.* **2013**, *42*, 7571–7637. [CrossRef] [PubMed]
15. Baláž, P. Mechanochemistry in minerals engineering. In *Mechanochemistry in Nanoscience and Minerals Engineering*; Springer: Berlin/Heidelberg, Germany, 2008; pp. 257–296.
16. Meng, F.; Li, H.; Zu, H.; Yang, J.; Yang, Z.; Qu, W. Mechanochemical activation of natural metal sulfide minerals for Vapor-Phase mercury immobilization. *Sep. Purif. Technol.* **2023**, *326*, 124710. [CrossRef]
17. Hao, J.; Liu, J.; Gao, H.; Yu, Y.; Bai, X. Auxiliary depression of copper ion-strengthening the depression of sodium trithiocarbonate on chalcopyrite. *Miner. Eng.* **2023**, *204*, 108395. [CrossRef]
18. Nadirov, R.K.; Turan, M.D.; Karamyrzayev, G.A. Copper ammonia leaching from smelter slag. *Int. J. Biol. Chem.* **2019**, *12*, 135–140. [CrossRef]
19. Meshram, P.; Prakash, U.; Bhagat, L.; Abhilash Zhao, H.; van Hullebusch, E.D. Processing of waste copper converter slag using organic acids for extraction of copper, nickel, and cobalt. *Minerals* **2020**, *10*, 290. [CrossRef]

Disclaimer/Publisher's Note: The statements, opinions and data contained in all publications are solely those of the individual author(s) and contributor(s) and not of MDPI and/or the editor(s). MDPI and/or the editor(s) disclaim responsibility for any injury to people or property resulting from any ideas, methods, instructions or products referred to in the content.